www.czasopisma.pan.pl PAN POLSKA AKADEMIA NAUK www.journals.pan.pl

PAN ARCHIVES OF ACOUSTICS
Vol. 41, No. 3, pp. 499–505 (2016)

DOI: 10.1515/aoa-2016-0048

Feedforward Control of a Light-Weight Device Casing for Active Noise Reduction

Stanislaw WRONA, Marek PAWELCZYK

Institute of Automatic Control
Silesian University of Technology
Akademicka 16, 44-100 Gliwice, Poland; e-mail: {stanislaw.wrona, marek.pawelczyk}@polsl.pl

(*received March 10, 2016; accepted April 5, 2016*)

It is possible to enhance acoustic isolation of the device from the environment by appropriately controlling vibration of a device casing. Sound insulation efficiency of this technique for a rigid casing was confirmed by the authors in previous publications. In this paper, a light-weight casing is investigated, where vibrational couplings between walls are much greater due to lack of a rigid frame. A laboratory setup is described in details. The influence of the cross-paths on successful global noise reduction is considered. Multiple vibration actuators are installed on each of the casing walls. An adaptive control strategy based on the Least Mean Square (LMS) algorithm is used to update control filter parameters. Obtained results are reported, discussed, and conclusions for future research are drawn.

Keywords: active control; flexible structures; active noise control; active vibration control; active structural acoustic control; active casing.

1. Introduction

An excessive noise generated by devices and machinery tends to become the subject of high interest to customers, producers and scientists. Prolonged exposure to a high-level noise, as in some industrial environments, can lead to hearing damage. In turn, domestic appliances can also be a source of noise, causing annoyance and significantly obstructing work or leisure. A classical protection solution is to apply passive sound insulating materials. However, passive barriers are often ineffective, especially at low frequencies, or are inapplicable due to increase in size and weight of the device, and its potential overheating. An alternative way is to use active control methods, by applying a set of sensors and actuators, and running a control algorithm driving secondary sources (Bismor *et al.*, 2016; Lorente *et al.*, 2015a; 2015b). Different control strategies were examined over the years (Mazur, Pawelczyk, 2013; 2016). The sound radiation of an individual elastic plate and other barriers was analyzed, e.g. in (Klamka *et al.*, 2015; Rdzanek, 2015; Zawieska, Rdzanek, 2014; Zhou, Crocker, 2010).

If a device generating noise is surrounded by a thin-walled casing, or if it can be enclosed in an additional casing, control inputs can be applied directly to the structure, and as a whole it can be used as an active barrier enhancing acoustic isolation of the device (Fuller *et al.*, 1994). Such approach is referred to as the active casing approach, and was further developed by the authors and successfully applied in previous research (Wrona, Pawelczyk, 2014; 2015). It results in a global noise reduction instead of local zones of quiet when appropriately implemented.

In previous research, when a rigid casing was used, each wall of the casing was vibrationally isolated from other walls, what simplified the problem of an active control. In the following research a cuboid light-weight casing is used. An important complication is that the walls of the casing are connected directly, without a rigid frame, what significantly augments vibration coupling between the walls. Hence, the influence of the cross-paths on successful global noise reduction is evaluated and discussed.

The intention of this paper is to further develop the active casing approach, by applying it for the light-weight casing. The laboratory setup is described in details. A high number of control inputs is considered, which requires a considerable computational power to implement a control system according to real-time constrains. Therefore, a relatively simple control strategy is adopted, where each wall is controlled separately

(as a first attempt of active control of the light-weight casing). The advantages and limits of such approach are pointed out and discussed.

The paper is organized as follows. Firstly, in Sec. 2 the laboratory setup of the light-weight active casing is described. Then, in Sec. 3 an Active Structural Acoustic Control (ASAC) system using a feedforward adaptive control strategy with the Normalised Leaky FxLMS algorithm is presented. Subsequently, in Sec. 4 results of the active control experiment are given. Finally, obtained results are discussed and conclusions for future research are drawn.

2. The laboratory setup

In this section, firstly the vibrating structure itself is described. Then, sensors and actuators are considered, along with a configuration of the whole laboratory setup in the view of control-related problems.

2.1. Vibrating structure: the light-weight device casing

The light-weight device casing used in this paper is a second type of casings investigated by the authors in a role of an active casing. The structure is presented in Fig. 1. In contrast to a rigid casing used in the previous research (e.g. in (Wrona, Pawelczyk, 2014; 2015)), the light-weight casing is made without an explicit frame. It is made of 1.5 mm steel plates

Fig. 1. Photographs of the light-weight active casing: a) from the outside, b) from the inside.

bolted together, forming a closed cuboid of dimensions $500 \times 630 \times 800$ mm. Such structure results in greater vibrational couplings between individual walls, in addition to couplings through the acoustic field inside and, to a lesser extends, outside the casing. Moreover, due to the absence of the rigid frame, the walls are connected directly to each other, what results in boundary conditions which no longer behave as fully-clamped (boundary conditions elastically restrained against both rotation and translation are more appropriate).

2.2. Sensors and actuators

In this stage of research, a loudspeaker placed on the floor with a sound-insulating basis is used as the primary noise source. It allows for creating an environment more suitable for the research than a real operating device, which will be used in due course. Vibration isolation between the speaker and the floor is provided to ensure only acoustic excitation of the casing.

For the feedfoward control system implementation, the reference signal is obtained by a microphone placed next to the loudspeaker inside the casing enclosure (referred to as the reference microphone). In front of each casing wall, a microphone is placed in the distance of 500 mm (referred to as the error microphone). These microphones are used for control-related purposes. Additionally, to evaluate the noise reduction efficiency, three microphones are placed at several larger distances from the casing, corresponding to potential locations of the user (referred to as the room microphones). A schematic representation of the laboratory setup is presented in Fig. 2.

To control vibrations of the active casing, inertial actuators EX-1 are used (presented in Fig. 3). They are light-weight (115 g) actuators of small dimensions (70 mm), comparing to the size of the casing. They are mounted on the casing walls from the inner side. Four actuators are used per front, right, back and left wall. For the largest top wall, five actuators are used. The number of actuators and their placement is a result of analysis and optimization using a method that maximizes a measure of the controllability of the system. The impact of the mass of the actuators is included in the optimization procedure. The method and mathematical model of casing walls are described in details in other publications of the authors (Wrona, Pawelczyk, 2016a; 2016b; 2016c).

The active casing described in this section is a three-dimensional structure. The couplings between individual walls, of both vibrational and acoustical nature, are significant. However, what is validated in (Wrona, Pawelczyk, 2016a), observed natural frequencies and modeshapes of the whole structure are a consequence of superposition of resonances of each wall excited individually (but as a part of the structure). Moreover, an impact of vibrations of one wall

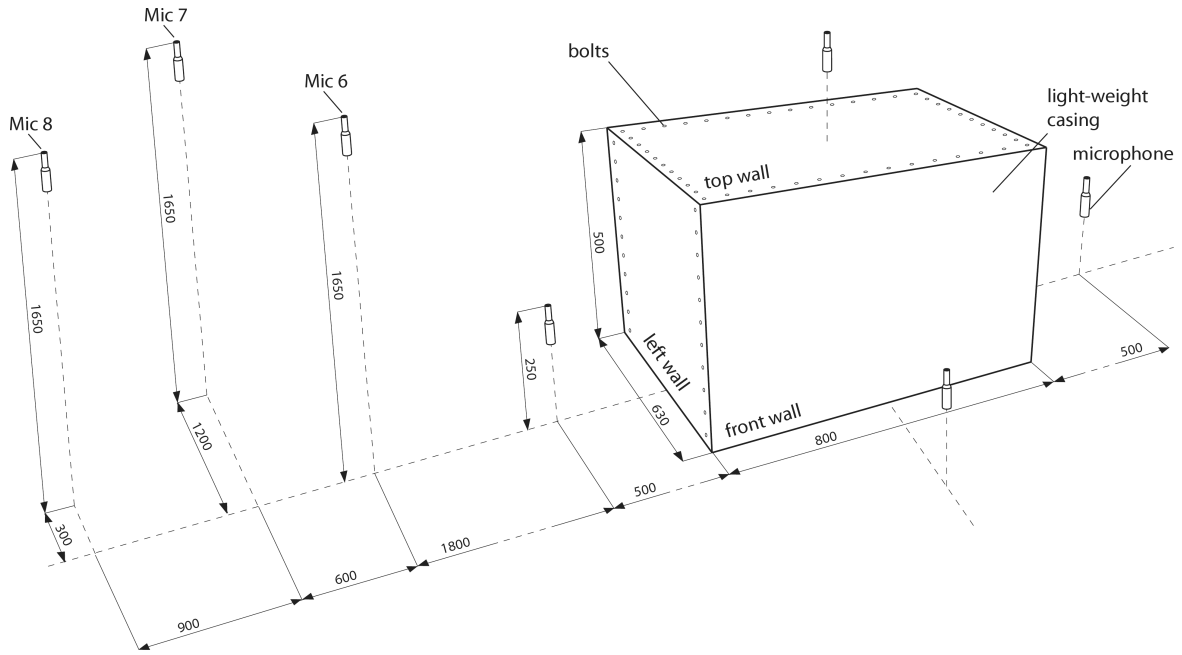

Fig. 2. A schematic representation of the laboratory setup. All dimensions are given in millimeters [mm].

Fig. 3. A photograph of an actuator mounted to the casing.

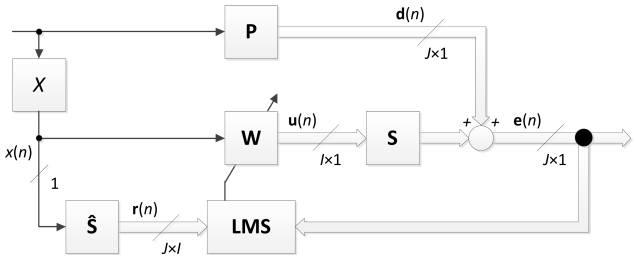

Fig. 4. Multi-channel feedforward control system with the FxLMS algorithm.

due to actuators mounted on another wall is significantly weaker for low frequencies (up to 250 Hz, as showed in (Mazur, Pawelczyk, 2016)), than the impact of actuators mounted directly on the wall. Therefore, to simplify the algorithm and reduce computational complexity, in this research a control strategy with each wall controlled separately is evaluated.

3. Adaptive control strategy

In this section, a multi-channel control system is presented, which is used in experiments described in the following section. It is an adaptive feedforward control strategy, based on the Leaky Normalised Filtered-x Least Mean Square (FxLMS) algorithm used to update control filter parameters. The adaptivity is introduced to respond to possible nonstationarity of the disturbance and changes of the plant, e.g. due to temperature variation (Mazur, Pawelczyk, 2011).

The control algorithm is schematically presented in Fig. 4. Signals $\mathbf{d}(n)$ and $\mathbf{e}(n)$ are the primary disturbances vector and the error signals vector (both of dimension $(J \times 1)$, where J is the number of error sensors), respectively, at positions of the error sensors where noise reduction is required. Further, $x(n)$ is the scalar reference signal, $\mathbf{r}(n)$ is the filtered-reference signals matrix (of dimension $(J \times I)$, where I is the number of actuators), $\mathbf{u}(n)$ is the control signals vector of dimension $(I \times 1)$. In turn, $\mathbf{W}$ is the adaptive control filters vector of dimension $(I \times 1)$, X is the reference path, figure $\mathbf{P}$ is the primary paths vector of dimension $(J \times 1)$, defined between the reference and error sensors, and $\mathbf{S}$ stands for the secondary paths matrix of dimension $(J \times I)$ defined between the inputs of the actuators and outputs of the error sensors. These paths include electronics necessary for signal conditioning and data conversion. The symbol $\widehat{\mathbf{S}}$ stands for the secondary path model. Depending on particular wall, the control system for the wall uses the number of actuators $I = 4$ or $I = 5$. On the other hand, the number of error sensors is $J = 1$, since in this paper one error microphone is used per wall.

The i-th control signal at the $(n+1)$-st sample, $u_i(n+1)$, is obtained as follows:

$$u_i(n+1) = \mathbf{w}_i(n)^{\mathrm{T}}\mathbf{x}_u(n), \tag{1}$$

where $\mathbf{x}_u(n) = [x(n), x(n-1), \ldots, x(n-(N-1))]^{\mathrm{T}}$ is the vector of regressors of the reference signal and $\mathbf{w}_i(n) = [w_{i,0}(n), w_{i,1}(n), \ldots, w_{i,N-1}(n)]^{\mathrm{T}}$ is the vector of coefficients of the i-th adaptive Finite Impulse Response (FIR) control filter at sample n, and N is the filter order. These coefficients are updated for each of the error signals $e_j(n)$ according to the formula:

$$\mathbf{w}_i(n+1) = \alpha\mathbf{w}_i(n) - \mu(n)\mathbf{r}_{ij}(n)e_j(n), \tag{2}$$

where $\mathbf{r}_{ij}(n) = [r_{ij}(n), r_{ij}(n-1), \ldots, r_{ij}(n-(N-1))]^{\mathrm{T}}$ is a vector of regressors of the ij-th filtered-reference signal, $\mu(n)$ is a step-size, and $0 \ll \alpha < 1$ is the leakage coefficient. The filtered-reference signal is calculated as:

$$r_{ij} = \widehat{\mathbf{s}}_{ij}(n)^{\mathrm{T}}\mathbf{x}_r(n), \tag{3}$$

where $\widehat{\mathbf{s}}_{ij}(n) = [\widehat{s}_{ij,0}(n), \widehat{s}_{ij,1}(n), \ldots, \widehat{s}_{ij,M-1}(n)]^{\mathrm{T}}$ is the vector of coefficients of the M-th order FIR model of the ij-th secondary path and $\mathbf{x}_r(n) = [x(n), x(n-1), \ldots, x(n-(M-1))]^{\mathrm{T}}$ is a vector of regressors of the reference signal.

4. Experimental results

In this section, experimental results for the light-weight casing are presented. All walls of the casing are controlled to reduce the emission of noise generated by a primary noise source enclosed in the casing. To achieve this goal, instantaneous square values of error signals are minimized by feedforward adaptive

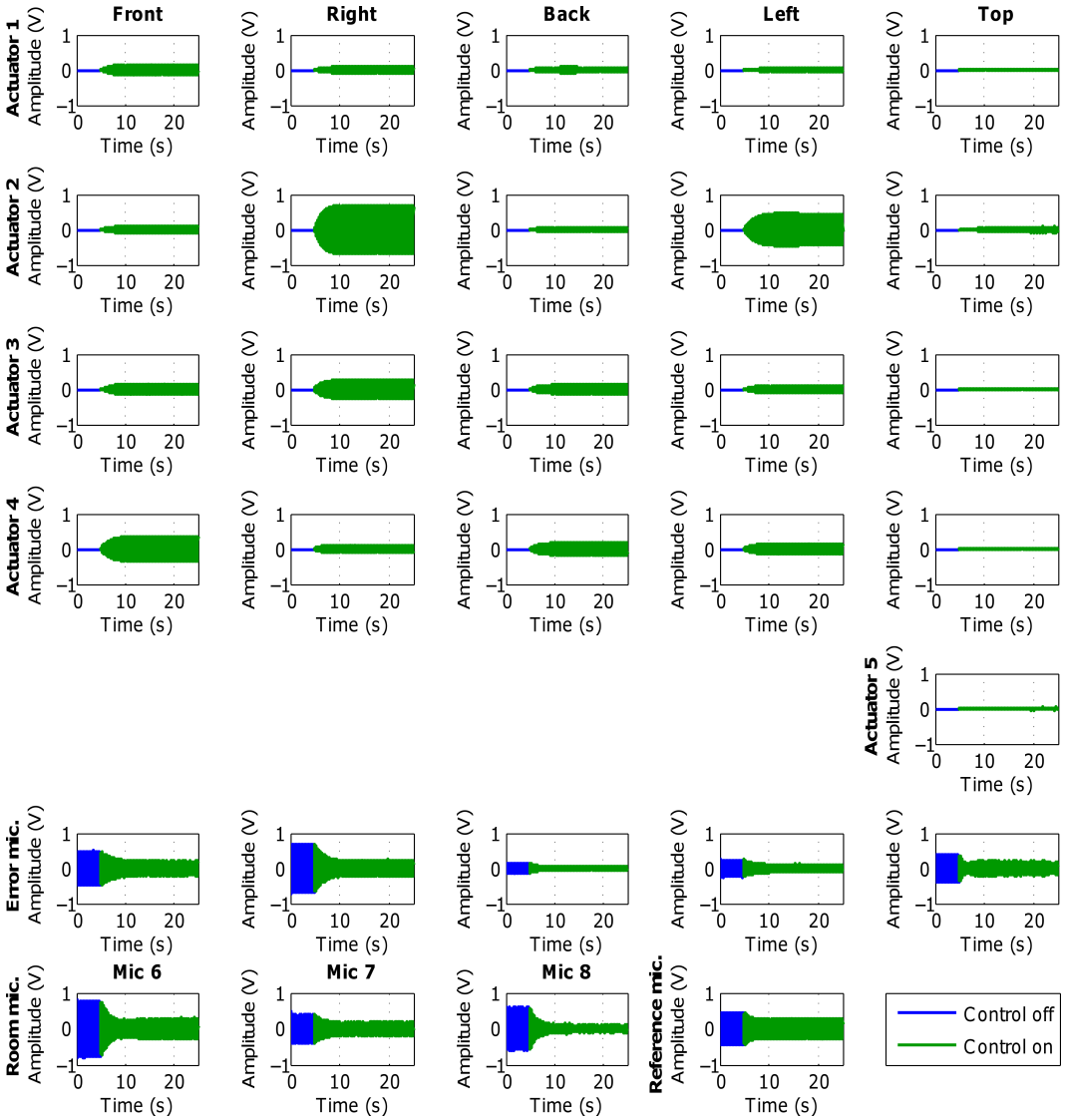

Fig. 5. Time plots for experiment performed for the primary disturbance of 214 Hz and the light-weight casing. The error microphones are used as error sensors.

ASAC systems, controlling twenty one inertial actuators (four per front, right, back and left wall, and five for the top wall). The error signal is obtained by the error microphones. The primary disturbance is generated as a tonal signal of frequency incremented by 1 Hz in the range from 15 Hz to 300 Hz. The considered frequency range includes the low frequencies where the speaker starts to transmit sound, up to higher frequencies (above 250 Hz) where the cross-paths between different walls become significant, thus the independent control provides weaker performance than for lower frequencies (even the entire system may become unstable). This issue can be mitigated using the Switched-error FxLMS algorithm, what is considered in other publications, e.g. in (Mazur, Pawelczyk, 2015) or (Mazur, Pawelczyk, 2016). However, it is noteworthy that these strategies require more computational power.

The control performance is evaluated as noise reduction level observed by all microphones. For each frequency of the primary disturbance, a 25 seconds experiment was performed. During its initial 5 seconds the active control was off, and variance of the signal acquired by different sensors was estimated. Then, active control was turned on. When the control algorithm converged, final 5 seconds of the experiment were used to estimate the variance of the signal acquired by corresponding sensors.

Results of an exemplary experiment in the time domain are presented in Fig. 5. First five rows present control signals, where the convergence rate can be observed. In the sixth row, signals measured by microphones used in this experiment as error sensors are shown. In the seventh row of the figure, signals measured by three room microphones are presented. The reference microphone measurement is also shown for completeness.

In Fig. 6 frequency characteristics for the experiment with feedforward control system are presented. In the last row of the figure, the mean reduction obtained at all microphones is shown. It is considered as the main point for evaluation of active control performance. Remaining plots present variances in dB scale of signals acquired by error sensors and individual room microphones, without (blue) and with (green) control. Additionally, bellow each individual frequency characteristic, a reduction characteristic is also presented, calculated as a difference between noise level without and with control (reduction is marked with red colour).

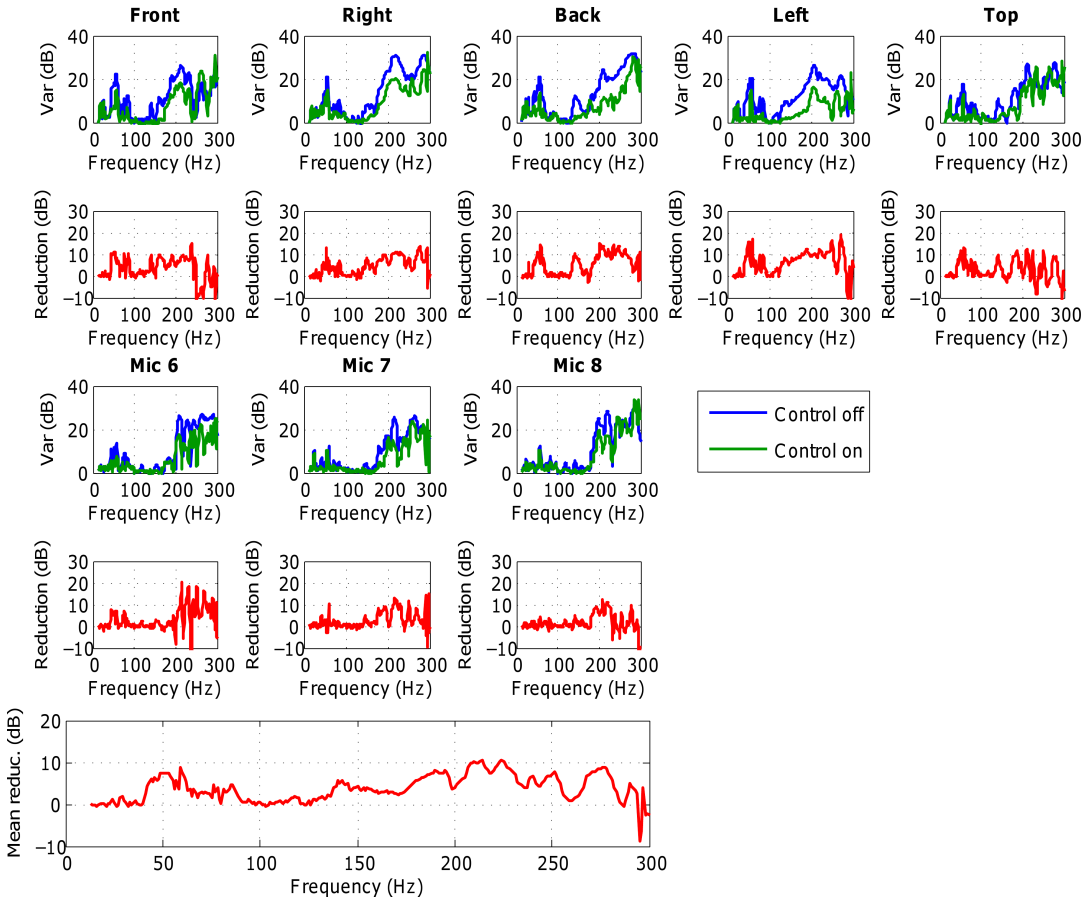

Fig. 6. Frequency characteristics for the experiment performed for the light-weight casing. The error microphones are used as error sensors.

5. Conclusions

Active structural acoustic control of multiple walls of the light-weight device casing has been performed. The feedforward adaptive ASAC system with the Normalised Leaky FxLMS algorithm has been used. Its performance has been evaluated for multiple microphones in the room. Significant levels of global noise reduction have been obtained (achieving 10 dB), confirming high potential of the active casing approach to reduce excessive device noise (even when a relatively simple control strategy has been employed – independent control system for each casing wall) (Wiora *et al.*, 2016).

The evaluated configuration performed well for low frequencies (up to 250 Hz), where the impact of vibrations of one wall due to actuators mounted on another wall is significantly weaker than the impact of actuators mounted directly on the wall. Its performance was reliable and noise enhancement or convergence problems never occurred. Hence, given control strategy achieve significant global noise reduction, with relatively low complexity of the system, where each wall is controlled separately. However, for frequencies above 250 Hz, the cross-paths between different walls become significant, and hence the independent control provides weaker performance (even the entire system may become unstable). This issue can be mitigated, however, by using more sophisticated strategies, e.g. the Switched-error FxLMS algorithm (Mazur, Pawelczyk, 2015), especially with the Virtual Microphone Control modification (Mazur, Pawelczyk, 2016). In future research the authors intend to develop these techniques further to improve global noise reduction. The active casing idea can also be extended by appropriately including energy recovery issues (Konieczny *et al.*, 2013; Kowal *et al.*, 2008).

Acknowledgments

The authors are indebted to two anonymous reviewers for their precious comments and suggestions, which helped improving the paper.

The research reported in this paper has been supported by the National Science Centre, Poland, decision no. DEC-2012/07/B/ST7/01408.

References

1. Bismor D., Czyz K., Ogonowski Z. (2016), *Review and comparison of variable step-size LMS algorithms*, International Journal of Acoustics and Vibration, **21**, 1, 24–39.

2. Fuller C.R., McLoughlin M.P., Hildebrand S. (1994), *Active acoustic transmission loss box*, PCT Patent WO 94/09484.

3. Klamka J., Wyrwal J., Zawiski R. (2015), *Mathematical model of the state of acoustic field enclosed within a bounded domain*, [in:] Methods and Models in Automation and Robotics (MMAR), 2015 20th International Conference on, 191–194.

4. Konieczny J., Kowal J., Raczka W., Sibielak M. (2013), *Bench tests of slow and full active suspensions in terms of energy consumption*, Journal of Low Frequency Noise, Vibration and Active Control, **32**, 1–2, 81–98.

5. Kowal J., Pluta J., Konieczny J., Kot A. (2008), *Energy recovering in active vibration isolation system – results of experimental research*, Journal of Vibration and Control, **14**, 7, 1075–1088.

6. Lorente J., Antonanzas C., Ferrer M., Gonzalez A. (2015a), *Block-based distributed adaptive filter for active noise control in a collaborative network*, [in:] Signal Processing Conference (EUSIPCO), 2015 23rd European, 310–314.

7. Lorente J., Ferrer M., de Diego M., Gonzalez A. (2015b), *The frequency partitioned block modified filtered-x NLMS with orthogonal correction factors for multichannel active noise control*, Digital Signal Processing, **43**, 47–58.

8. Mazur K., Pawelczyk M. (2011), *Active noise-vibration control using the filtered-reference lms algorithm with compensation of vibrating plate temperature variation*, Archives of Acoustics, **36**, 1, 65–76.

9. Mazur K., Pawelczyk M. (2013), *Active noise control with a single nonlinear control filter for a vibrating plate with multiple actuators*, Archives of Acoustics, **38**, 4, 537–545.

10. Mazur K., Pawelczyk M. (2015), *Multiple-error adaptive control of an active noise-reducing casing*, [in:] Progress of Acoustics, 701–712.

11. Mazur K., Pawelczyk M. (2016), *Virtual microphone control for a light-weight active noise-reducing casing*, [in:] Proceedings of 23th International Congress on Sound and Vibration.

12. Rdzanek W.P. (2015), *Total acoustic power of two concentric clamped circular plates vibrating in a fluid*, Acta Physica Polonica A, **128**, 1A, A41–A45.

13. Wiora J., Kozyra A., Wiora A. (2016), *A weighted method for reducing measurement uncertainty below that which results from maximum permissible error*, Measurement Science and Technology, **27**, 3.

14. Wrona S., Pawelczyk M. (2014), *Active reduction of device multi-tonal noise by controlling vibration of multiple walls of the device casing*, [in:] Proceedings of 19th International Conference on Methods and Models in Automation and Robotics (MMAR), IEEE, Miedzyzdroje, Poland, 2–5 September.

15. Wrona S., Pawelczyk M. (2015), *Active reduction of device narrowband noise by controlling vibration of its*

casing based on structural sensors, [in:] Proceedings of 22nd International Congress on Sound and Vibration, Florence, Italy, 12–16 July.

16. Wrona S., Pawelczyk M. (2016a), *Optimal placement of actuators for active structural acoustic control of a light-weight device casing*, [in:] Proceedings of 23th International Congress on Sound and Vibration.

17. Wrona S., Pawelczyk M. (2016b), *Shaping frequency response of a vibrating plate for passive and active control applications by simultaneous optimization of arrangement of additional masses and ribs. Part I: Modeling*, Mechanical Systems and Signal Processing, **70–71**, 682–698.

18. Wrona S., Pawelczyk M. (2016c), *Shaping frequency response of a vibrating plate for passive and active control applications by simultaneous optimization of arrangement of additional masses and ribs. Part II: Optimization*, Mechanical Systems and Signal Processing, **70–71**, 699–713.

19. Zawieska W., Rdzanek W. (2006), *Low frequency approximation of mutual modal radiation efficiency of a vibrating rectangular plate*, Archives of Acoustics, **31**, 4 (Supplement), 123–130.

20. Zhou R., Crocker M.J. (2010), *Sound transmission characteristics of asymmetric sandwich panels*, Journal of Vibration and Acoustics, **132**, 3.